A Parameterization for the Shortwave Transmissivity of Stratiform Water Clouds Based on Empirical Data and Radiative Transfer Theory

V. E. DERR,* R. S. STONE,† L. S. FEDOR‡ AND H. P. HANSON†

* *NOAA, Environmental Research Laboratories, Boulder, Colorado*
† *Cooperative Institute for Research in Environmental Sciences, University of Colorado/NOAA, Boulder, Colorado*
‡ *NOAA/ERL, Wave Propagation Laboratory, Boulder, Colorado*

(Manuscript received 16 November 1989, in final form 12 June 1990)

ABSTRACT

Surface measurements of solar flux and total integrated liquid-water content, radiosonde data, and infrared satellite images are analyzed in conjunction with radiative transfer calculations to derive an empirical parameterization for the shortwave transmissivity of continental stratiform water clouds. The data were collected near Denver, Colorado, over a period of six years. Seventeen days on which uniform stratiform clouds persisted over the observing site were selected for detailed analysis, and form the basis for deriving the parameterization. A multiple reflection radiative transfer model is employed to estimate stratus cloud transmissivity in terms of the measurable liquid-water path (LWP). A nonlinear fit of estimated transmissivities to the corresponding observations of LWP yields close agreement with a previous, more complicated parameterization. The derived expression for cloud transmissivity is used to predict mean daily surface fluxes for 61 days during which periods of stratiform clouds were observed over the Denver area. A comparison between predicted and measured fluxes shows agreement to within ±4%, with best agreement for clouds of moderate optical thickness. Potential sources of error are identified with sensitivity studies.

1. Introduction

Water, in all its phases, plays a crucial role in interactions with radiation in the atmosphere. Clouds, in particular, profoundly affect the reflection, transmission, and absorption of sunlight entering the atmosphere, thereby radiatively forcing the earth–atmosphere energy balance. Recent analysis by Ramanathan et al. (1989) of data collected as part of the Earth Radiation Budget Experiment (ERBE) indicates that the net radiative forcing by clouds may be four times greater than that predicted for a global doubling of CO_2. Therefore, even small changes in cloud amount or character on a global scale could lead to significant climate perturbations. Depending on how clouds interact with atmospheric dynamics and sensible and latent heat exchanges, changes in cloud distributions could contribute to either an increase or a decrease in global temperatures. Dealing with these nonlinear feedback processes remains a difficult problem.

One formidable problem is to simulate accurately the surface energy budget under the influence of clouds, which typically vary in space and time. To accomplish this on a global scale, simple yet accurate parameterizations of the bulk radiative properties of various cloud types are needed for use in general circulation models (GCMs). Such parameterizations have been developed from theoretical considerations by Stephens (1978), Stephens et al. (1984), Liou and Wittman (1979), and more recently Slingo (1989), among others. Each of these methods uses as its primary independent variable the cloud liquid-water path (LWP), the amount of cloud water integrated along a path aligned with the solar zenith angle. The use of LWP is favored for two reasons: 1) both shortwave optical depth and longwave emissivity can be related to the total water–ice content of a cloud integrated along this path (Stephens 1978), and 2) LWP can be measured from operational satellites equipped with microwave radiometers to an accuracy of 0.01 g cm^{-2} in most circumstances (Staelin et al. 1976; Pandey et al. 1983).

In this study we analyze surface-based measurements of solar flux and integrated liquid-water content in combination with auxiliary data from routine weather observations and satellite imagery. Analysis of these data in conjunction with simple theoretical calculations is used to derive empirically a parameterization for stratus cloud transmissivity in terms of LWP. Because our dataset does not include measurements of reflected solar flux, the parameterization for stratus albedo developed by Stephens et al. (1984) is implemented as part of our analysis to deduce stratus cloud tramsmissivity.

Unlike the theoretical schemes mentioned above, which assume idealized horizontally homogeneous cloud layers within model atmospheres, we use a large body of empirical data measured continuously over a

Corresponding author address: Vernon E. Derr, NOAA/ERL, 325 S. Broadway, R/E, Boulder, CO 80303.

period of six years to deduce the transmission properties of stratus clouds. Such an approach inherently takes into consideration much of the spatial and temporal inhomogeneity that has been observed in stratiform cloud systems (Derr and Hanson 1984).

2. Experimental design

The analysis presented here is based on measurements taken over a 6-year period (1983–1988) at a site adjacent to the Weather Service Field Office (WSFO) at the Stapleton International Airport in Denver, Colorado. The principal measurements used in this analysis are the downward solar flux at the ground F_g and the total vertical atmospheric integrated liquid-water content (ILWC). WSFO surface observations, including radiosonde data and the total sky cover, in conjunction with GOES infrared (IR) satellite imagery and radiosonde data, are used to determine cloud cover and estimate cloud heights, thicknesses, and temperatures.

The broadband solar flux was measured by an upward-facing Eppley pyranometer mounted 3 m above the ground and having a spectral response between 0.4 and 2.8 μm and a hemispheric field of view (FOV). This instrument was routinely calibrated at the NOAA Solar Radiation Facility (SRF) in Boulder, Colorado, against a standard instrument referenced to a cavity radiometer. It is accurate to within ±5% (Dutton et al. 1985), but under cloudy conditions, uncertainties due to direct beam angular effects are reduced by about 2.5%; thus, overall accuracy under stratiform cloud conditions is expected to be within about ±3% (see also Meyers 1987).

ILWC and water-vapor profiles were derived from the 31.65 and 20.6 GHz channels of a zenith-pointing microwave radiometer as described by Hogg et al. (1983). This radiometer measures total column ILWC within a 6° beamwidth with a sensitivity of about 0.1 mm and has an rms accuracy of 10% for nonprecipitating clouds. It was routinely calibrated by reference to a temperature-controlled load (refer to Askne and Westwater 1986; Hogg et al. 1983, for details). Because no direct measurements of cloud ice content were made, data were analyzed only for near-summer months to minimize the effects of ice on calculated transmissivity.

Figure 1 shows typical cloudy day signals of the four primary variables on which the analysis is based: F_g, ILWC, the correlation between F_g and ILWC, and cloud cover (CC). Two-minute average values of F_g, ILWC, and their correlation are shown. F_g and ILWC were used to compute a sliding correlation estimate based on a 1-h integration interval. These mean values of correlation were used as an indicator of cloud homogeneity. In order to assure a reasonable degree of cloud homogeneity, only data with correlation less than −0.8 are analyzed here. Figure 1 shows this anticorrelation clearly. Cloud cover data were taken directly from the WSFO hourly sky cover reports.

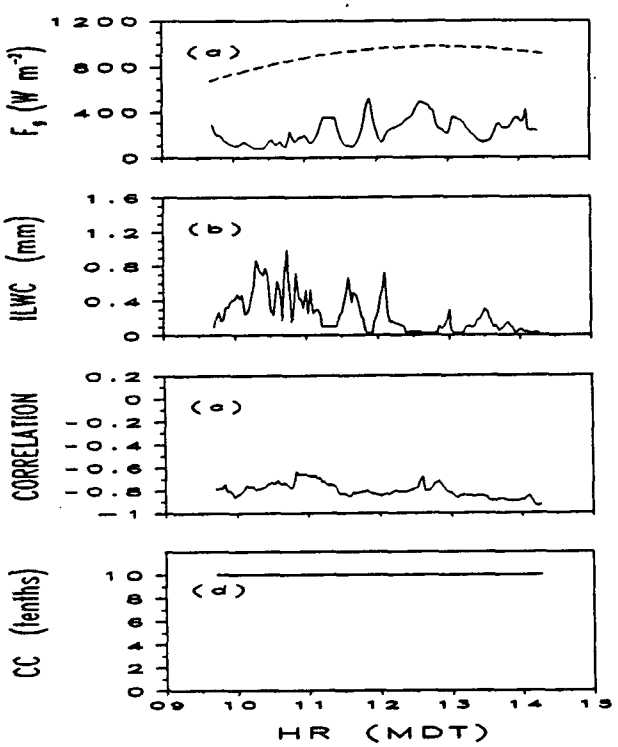

FIG. 1. Two-minute average values of (a) surface flux F_g, (b) total integrated liquid-water content ILWC, (c) correlation between F_g and ILWC, and (d) hourly cloud cover CC for a typical cloudy day during the Denver Stratus Experiment. The dashed curve in (a) shows the clear-sky flux for a previous day.

Although the ideal cloud-radiation experiment has yet to be undertaken, we were fortunate in this particular study to have a long and continuous record of pertinent measurements for analysis. The field instruments were well maintained and calibrated regularly. A variety of cloudy conditions as well as totally clear days necessary for calibration checks are included in the dataset. The auxiliary data are especially useful for estimating the boundary conditions for use in the radiative transfer model. On the other hand, the experiment suffered from the lack of in situ measurements to confirm estimates of cloud-top flux, determine cloud dropsize distributions, and verify the existence of cloud ice. Cloud heights and thicknesses were estimated from interpolated radiosonde data, and the radiative effects of clear-sky aerosols were estimated from nearby turbidity measurements. Perhaps the greatest potential source of error in interpreting the data results from the differences in the respective fields of view of the pyranometer and microwave radiometer. The sliding correlation estimate used to infer spatial and temporal homogeneity only ensures a high probability that the narrow FOV ILWC measurements are consistent with the simultaneous hemispheric flux measurements.

3. Theory

The theoretical basis we use for deriving stratus cloud transmissivity is a simple radiative transfer model described by Wiscombe (1975). It is a formulation of the two-stream approximation for radiative transfer through stratiform layers assumed to be uniformly distributed in the horizontal plane that accounts for multiple reflections between the surface and the cloud base. The model predicts the broadband solar flux incident at ground level, F_g (a list of symbols is found in the Appendix). The expression for F_g involves six variables: the downward radiative flux incident at cloud top (F_{ct}), the transmissivities of the cloud and subcloud layers (T_c and T_{cg}), and the albedos at cloud base, at the surface, and for the intervening atmosphere (α_d, ρ, and α_{cg}, respectively). A schematic of this multiple reflection model is presented in Fig. 2. Additional simplifications, for clarity, in Fig. 2 take T_{cg} to be unity and the cloud-base albedo α_d to be equal to the cloud-top albedo α_c. In this figure, a_c is the cloud absorptivity. F_g is given (after Wiscombe 1975) as

$$F_g = \gamma T_{cg} F_{ct}, \tag{1}$$

where

$$\gamma = \frac{T_c}{[(1 - \alpha_d\alpha_{cg})(1 - \rho\alpha_{cg}) - \rho\alpha_d T_{cg}^2]}.$$

In a comparison between this model and a detailed, 75 spectral interval, 12 stream, multiple-scattering model, Wiscombe showed that calculations of the ratio F_g/F_{ct} computed using the respective models generally agreed over a wide range of solar zenith angles and surface albedos. Thus, if the variables on the right-hand-side of Eq. (1) can be determined, reasonable estimates of surface flux can be made. These variables are not known a priori, however. Wiscombe parameterized them on the basis of results from his detailed model.

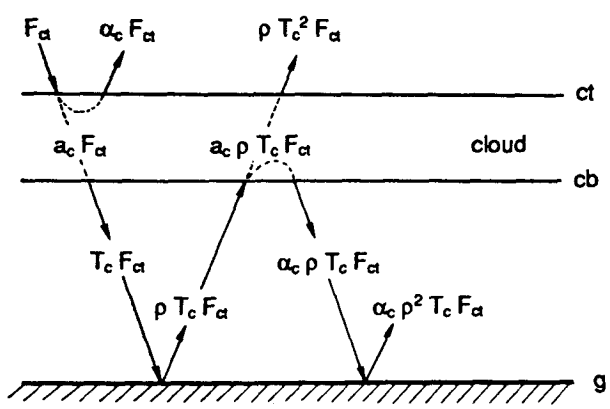

FIG. 2. Schematic of multiple reflections between a plane-parallel cloud layer and a reflective surface (after Wiscombe 1975), assuming 100% transmission below cloud base and identical cloud base and cloud top albedos.

Because we measured F_g and the corresponding values of ILWC and the zenith angle (θ_o), our objective here is to use (1) to calculate T_c using the known values of F_g and a parameterized relationship between cloud albedo and LWP [= ILWC/cos(θ_o)] to be discussed below; that is,

$$T_c = \frac{F_g}{T_{cg}F_{ct}}[(1 - \alpha_d\alpha_{cg})(1 - \rho\alpha_{cg}) - \rho\alpha_d T_{cg}^2], \tag{2}$$

where now $\alpha_d = f(\text{LWP})$. Therefore, based on measurements of F_g, we obtain T_c for real clouds by using a plane-parallel, multiple-reflection model and various approximations described below to determine the other unknowns.

The advantage of this approach lies in the use of a large dataset consisting of two of the most important variables that relate directly to solar attenuation; namely F_g and LWP. Such a body of data inherently includes a statistically significant range as a consequence of the natural inhomogeneity of clouds. Thus, an empirical analysis of these data is expected to lead to results that are climatologically significant and may be useful for climate simulation studies. Schemes based primarily on theoretical simulations involving idealized clouds, on the other hand, do not usually account for such natural variability.

Not all the relevant variables needed to solve (2) were measured during the course of the experiment. Determination of these quantities is discussed in the following section.

4. Empirical and theoretical analysis

A brief outline of the analysis procedure follows:

(1) Determine the unknown quantities on the right side of (2).

(2) Obtain 2-minute average values of T_c for a selected set of data, using (2).

(3) Plot corresponding values of T_c versus LWP.

(4) Fit the data to obtain a parameterization of T_c in terms of LWP.

a. Determination of model parameters

1) SIMULATION OF F_{ct} AND T_{cg}

Because no measurements of the flux incident at cloud top F_{ct} and the subcloud atmospheric transmissivity T_{cg} were obtained during our field experiment, these quantities were calculated using a radiative transfer model. This is possible providing the appropriate boundary conditions are known; these include the cloud height and thickness, the temperature and humidity profiles, and the solar geometry. We used the discrete-ordinate multiple-scattering model developed by Stamnes et al. (1988) for this purpose, employing a combination of radiosonde and satellite analyses to establish the necessary boundary conditions. Calcula-

tions were made over the spectral range 0.4–2.8 μm in order to match the filtered spectral response of the pyranometer. The model spectral resolution over this region is irregular and includes 18 narrow bands based on the exponential sum fitting of transmission data of Slingo and Schrecker (1982) (see Tsay et al. 1989, for details regarding the implementation of this model).

Days on which uniform, single-layer stratiform clouds were observed for several hours were selected for detailed analysis. Morning (0400 LST) and afternoon (1600 LST) temperature and humidity profiles showed marked similarity on such days, indicating that the state of the atmosphere remained reasonably stable over the periods of interest. Cloud-top and base heights were estimated from the interpolated radiosonde data, assuming that cloud filled the vertical region in which the relative humidity exceeded 90%. Seventeen cases (Table 1) were selected to represent a range of cloud thicknesses and heights typical of summertime stratus conditions along the Front Range of the Rockies. Some clouds with "cold" tops were intentionally selected in order to evaluate the sensitivity of calculated transmissivities to the presence of ice. Although no specific selections involving cirrus were made, some instances of cirrus were confirmed later by analyzing the corresponding GOES IR satellite images. The images, centered on the WSFO site, were analyzed at full resolution ($\sim 4 \times 8$ km) and statistics were estimated from the image IR temperatures over an area of 32 km^2. The statistical quantities used to determine the type of cloud coverage were the mean, standard deviation from the mean (SD), median (MED), and mode temperatures over this area (Table 2).

In each case the discrete-ordinate model was initialized for predetermined boundary conditions. The Sc I cloud model of Stephens (1979) was assumed to fill the cloud volume. Although an arbitrary choice, the Sc I model, prescribed as having a liquid water content of 0.14 g m^{-3} and an effective drop-size radius of 5.36 μm, is probably the best representation of mean stratiform cloud conditions during the summer months in the Rocky Mountain region. The solar flux at the top of the atmosphere was specified for each case in the simulations in order to account for seasonal differences in the sun–earth distance. A constant aerosol optical depth for the above-cloud layer of 0.02 was prescribed for all simulations. This value is typical for aerosol optical depths derived from sun photometer measurements made by the Geophysical Monitoring for Climatic Change division of NOAA at an altitude of about 3 km above mean sea level in the mountains NW of Stapleton Airport during the summer months.

Model simulations of cloud-top fluxes were used to derive quadratic relationships between F_{ct} and solar zenith angle. These relationships were subsequently used to predict F_{ct} at each 2-minute time step in order to estimate cloud transmissivity using (2). These computations used the Denver WSFO radiosonde measurements of humidity and temperature for each of the 17 cases. Simulations using the multiple scattering model of downward cloud-base flux F_b and downward surface flux F_s were used to obtain mean values for T_{cg} estimated by the ratio F_s/F_b for each period selected for analysis.

2) Approximation of the surface and sub-cloud albedos

No direct measurements of ρ or α_{cg} were obtained at the Stapleton site; therefore, these quantities were approximated. Surface albedo is routinely derived from continuous solar flux measurements obtained atop the 300 m Boulder Atmospheric Observatory (BAO) located about 50 km NNW of Stapleton Airport. The

TABLE 1. Mean values of measured and derived quantities for the 17 cases of stratiform clouds analyzed in this study.

Date (yr mo dy)	Number of 2-min averages	Cloud thickness (km)	Zenith angle θ_0 (degrees)	LWP (mm)	Sfc flux F_g (W m^{-2})	Correl. flux, ILWC	Cld top flux F_{ct} (W m^{-2})	Subcld trans T_{cg}	Parameterized α_c	Parameterized a_c	Parameterized T_c
83 05 11	79	1.35	27.9	0.324	140	−0.866	982	1.00	0.73	0.16	0.11
85 04 29	29	1.54	26.3	0.410	135	−0.829	1022	0.98	0.72	0.16	0.11
05 21	17	3.21	23.0	1.270	59	−0.844	1043	0.99	0.75	0.18	0.06
08 14	24	0.32	42.6	0.290	145	−0.864	767	0.98	0.74	0.13	0.14
09 20	40	1.17	46.1	0.262	167	−0.888	759	0.98	0.74	0.12	0.14
86 05 08	28	0.71	36.4	0.556	90	−0.852	878	1.00	0.75	0.16	0.09
05 29	30	1.34	34.6	0.677	197	−0.884	924	0.98	0.75	0.17	0.09
09 06	42	1.48	40.1	0.556	160	−0.853	847	1.00	0.76	0.15	0.09
87 05 21	34	1.32	33.1	0.246	184	−0.846	919	1.00	0.72	0.14	0.14
06 08	5	0.91	34.4	0.219	197	−0.826	921	0.99	0.71	0.14	0.15
06 29	34	3.13	28.4	1.324	86	−0.857	988	1.00	0.77	0.18	0.05
88 05 19	48	3.52	27.9	0.722	132	−0.836	990	1.00	0.75	0.18	0.07
05 20	17	2.26	31.1	0.246	160	−0.892	972	0.99	0.71	0.15	0.14
05 22	40	0.92	24.4	0.349	170	−0.838	1027	0.97	0.72	0.16	0.11
06 29	15	1.11	18.2	0.520	183	−0.829	1040	0.96	0.73	0.18	0.09
09 12	92	1.75	40.6	0.696	120	−0.871	850	1.00	0.77	0.16	0.08
09 13	95	1.23	43.5	0.342	135	−0.888	785	0.99	0.73	0.13	0.14

TABLE 2. Summary of satellite and radiosonde analysis of cloud heights and temperatures used to determine the presence of ice within or above stratiform clouds.

	Derived from radiosondes					Derived from GOES IR images							
Date (yr mo dy)	Top (K)	Hgt (km)	Base (K)	Hgt (km)	Surf (K)	Mean (K)	SD (°K)	Med (K)	Mode (K)	Max (K)	Min (K)	ΔT (°K)	Remarks
83 05 11	274	1.44	283	0.09	284	270	1.4	270	270	273	266	4	
85 04 29	267	2.79	282	1.25	284	231	3.0	230	230	244	227	cirrus	
05 21	259	4.14	278	0.93	286	224	5.4	222	221	244	218	35	cirrus
08 14	280	1.62	282	1.30	295	283	5.9	282	276	288	272	−3	
09 20	273	2.14	274	0.97	285	264	1.6	263	263	268	262	9	
86 05 08	270	0.94	276	0.23	279	253	4.1	253	254	262	246	17	cirrus
05 29	264	3.09	271	1.75	287	269	4.6	267	264	281	261	−5	ice
09 06	276	1.75	281	0.27	282	275	1.6	274	274	276	274	1	
87 05 21	273	1.72	279	0.40	282	267	3.4	266	266	276	258	6	
06 08	279	1.87	284	0.96	294	278	3.8	277	276	287	269	1	
06 29	267	3.32	286	0.19	288	233	7.6	231	234	252	223	34	cirrus
88 05 19	262	4.07	274	0.55	279	240	4.3	240	237	249	232	22	cirrus
05 20	261	3.19	274	0.93	281	239	6.3	237	235	257	228	22	cirrus
05 22	263	3.35	265	2.43	284	250	9.5	253	256	274	226	13	cirrus
06 29	266	4.59	272	3.48	296	268	10.0	267	267	289	243	−2	
09 12	272	1.96	278	0.21	280	248	6.2	246	243	265	240	24	cirrus
09 13	275	1.79	278	0.56	283	273	0.9	273	274	275	265	2	

Notes: Heights are above Mean Ground Level (MGL); SD = standard deviation; MED = median; $\Delta T = T_{\text{RAOB}} - T_{\text{GOES IR}}$.

topography and vegetation in the vicinity of the BAO tower and the WSFO station are sufficiently similar that the values of surface albedo derived for the tower location can be assumed to be representative of the region of interest here; thus, we use the BAO May–September mean albedo of 0.18 in our calculations (see Dutton 1989, for a detailed description of the data used to determine ρ). Because the surface albedo enters (2) only through multiple reflection terms, expected uncertainties in ρ do not lead to large errors in our final results.

Rayleigh and aerosol scattering in the clear atmosphere below the cloud base is expressed by α_{cg} in (2). Wiscombe's (1975) analysis indicated that α_{cg} was of the order of 0.5% and that it was rather insensitive to zenith angle for the range of interest here. Based on values of the total downward flux and the diffuse upward flux at the top of the subcloud layer calculated using the multiple scattering model described previously, we prescribed a mean value of 0.006 for α_{cg} for all of our transmissivity calculations.

3) PARAMETERIZATION OF α_d

Wiscombe (1975) also noted that the cloud-top albedo α_c and the diffuse cloud-base albedo α_d are nearly equal for solar zenith angles less than about 50°. Because the mean zenith angle for our case studies was about 35°, we assume that $\alpha_d = \alpha_c$ in our analysis and use a previously derived parameterization of broadband cloud albedo developed by Stephens (1978) and Stephens et al. (1984) to estimate α_c. This parameterization uses cloud liquid water in a manner consistent with our measurements; we also used the Sc I model in the parameterization, as described above.

b. Parameterization of T_c

After the quantities on the right-hand-side of Eq. (2) were determined, cloud transmissivity was calculated from that expression. Two-minute average values were calculated for all data on the 17 selected days that met the following criteria:

(1) ILWC > 0.004 cm (to eliminate noisy data)
(2) F_g, ILWC correlation < −0.8 (to assure a degree of horizontal homogeneity)
(3) CC > $^8/_{10}$ (to ensure cloudy conditions)
(4) Solar zenith angle < 55° (to reduce uncertainties associated with angular effects in the measurement of F_g).

Given data points that meet these criteria, parameterizing T_c in terms of the LWP involves choosing an appropriate functional form for the parameterization and then performing the appropriate numerical regression. Coakley and Snider (1989a,b) discussed this problem from the perspective of a dataset consisting of measurements of LWP and cloud albedo; they concluded that two-stream theory justifies the use of a function of the form

$$1/\alpha_c = A + B/\text{LWP}. \tag{3}$$

This is readily apparent when the *nonabsorbing* form of the two-stream approximation is used (e.g., Stephens 1978). If the two-stream approximation for an *ab-*

sorbing medium is used, the first terms of a series expansion of the absorptivity give a similar functional form. This form has several attractive features, including well-behaved extremes (so that both albedo and absorptivity are zero for LWP = 0 and asymptote to a maximum value for large LWP) and computational simplicity.

That this functional form is appropriate can be shown by using it to develop an expression for the cloud albedo α_c directly from the Stephens et al. (1984) parameterization, which uses polynomial regressions for the single-scattering albedo and the backscatter fraction in two bands in two-stream theory. If our measurements of ILWC and zenith angle (that is to say, the range of our observations) are used in the Stephens et al. two-stream parameterization, and the resulting albedos are regressed against LWP via (3), we obtain a very close fit, with $A = 1.24$ and $B = 0.037$ yielding a residual standard deviation of RSD = 0.014.

In parameterizing the transmissivity, we reason that the combined effects of reflection and absorption behave in a fashion qualitatively similar to the effect of either process alone, and therefore we can write the transmissivity as

$$T_c = 1 - \frac{1}{C + D/\mathrm{LWP}} \qquad (4)$$

where C and D are the new unknowns.

Figure 3 shows the observed transmissivities and results of a nonlinear least-squares regression to determine C and D in Eq. (4) (solid curve). The residual standard deviation of the parameterization for T_c for the 669 data points meeting the criteria listed above is RSD = 0.041 over a range of ILWC from 0.1 mm to 2.2 mm with $C = 1.062$ and $D = 0.038$. This range of LWP, for the zenith angles considered here, encompasses the useful range of sensitivity of the microwave radiometer. Table 1 lists the 17 cases used for this analysis and gives statistical information regarding the calculations, and Table 2 summarizes the WSFO and GOES data for these cases.

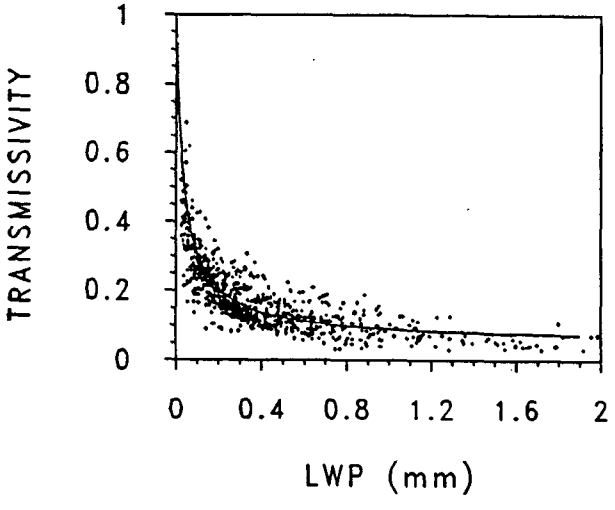

FIG. 3. Empirical fits for the calculated cloud transmissivities T_c as a function of liquid water path LWP obtained from Eq. (4). The scatter of points are those values for the 17 cases (669 2-minute averages) analyzed.

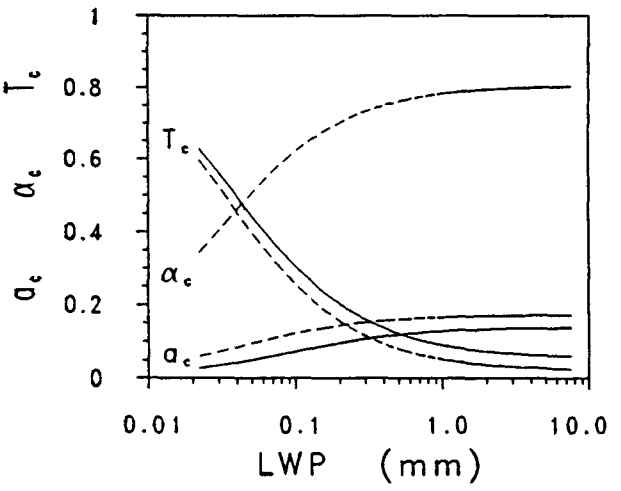

FIG. 4. Transmissivity as in Fig. 3, with results of Stephens et al. (1984) superimposed (dashed); the absorption curves are the Stephens et al. parameterization (dashed) and that inferred from Eqs. (3) and (4).

An evaluation of this method indicates that, for the mean cloud-top flux calculated, using the multiple scattering model of the 17 cases used here, of 904 W m^{-2} (assuming climatological values for the other unknown quantities), the surface flux can be predicted to within ±36 W m^{-2} by using (1) and the parameterizations for α_c and T_c in (3) and (4), respectively.

5. Validation and sensitivity analyses

a. Comparison with Stephens' parameterization

Figure 4 is presented for comparison with the theoretical results of Stephens et al. (1984). The curves are those presented in Fig. 3 for all 17 cases (solid). The results of Stephens et al. (1984) are given by the dashed curves. Note that the results presented here have been corrected to reflect the spectral interval (0.4–2.8 μm) measured by the pyranometer.

The notable differences between our empirically based results and those of Stephens et al. (1984) are that as the LWP becomes large, Stephens et al.'s transmissivities become increasingly lower than ours and their values for absorptivity remain consistently greater than ours over most of the range of LWP.

In the face of this consistency with other results, it must be noted that the sensitivity of these bulk cloud radiative properties to variations in cloud drop size

distributions is larger than the differences between theory and measurement discussed above (e.g., Slingo 1989). This underscores the need for coordinated measurements of radiative fluxes, cloud LWP, and cloud drop size distributions.

b. *Validation of the predictive model for surface flux*

To test the parameterizations for stratus cloud transmissivity and albedo described above, the six-parameter model [Eq. (1)] was used to derive a predicted downward surface flux F_p for all the days during the 6-year period in which stratiform clouds were observed over Denver. Again, only days between May and September were considered, to reduce the likelihood of ice contamination. The values of F_p are compared with the measured fluxes F_g in the form of the scatter plot presented in Fig. 5. Data used to compute the daily means consist of all 2-minute averages for solar zenith angles that were less than 85° and met the other criteria listed in section 4; 61 days on which stratiform clouds persisted for at least 30 minutes are included in this figure. Calculations were based on Eq. (1) with the assumption that the cloud-base albedo is equal to that at cloud top and with the transmissivity parameterization based on the 17 selected cases described earlier. In every case the surface and subcloud atmospheric albedos were prescribed to be 0.18 and 0.006, respectively (consistent with the previous analysis). "Climatological" values for T_{cg} and F_{ct} were used, assuming that these 17 cases were climatologically representative of typical summertime stratus clouds in the Denver region. Thus, T_{cg} was given the value of 0.98 and F_{ct} was estimated using a quadratic function relating simulated cloud-top fluxes to solar zenith angle determined by a fit of F_{ct} versus θ_o for the simulations already made.

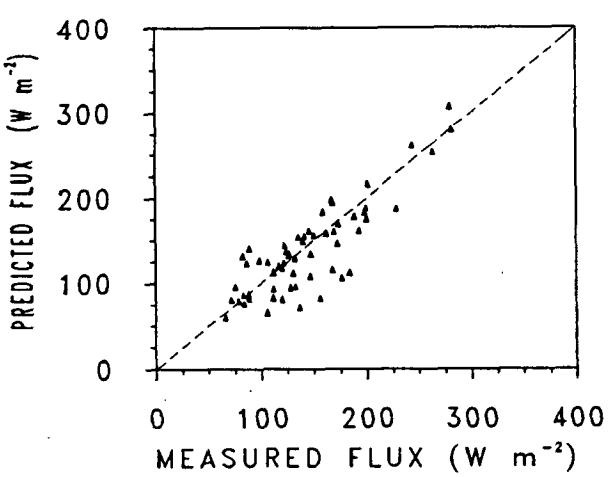

FIG. 5. Mean daily values of predicted versus measured surface flux for 61 days on which stratiform clouds were observed over Denver. The dashed line represents perfect agreement between predicted and measured values.

The residual standard deviation of fit of F_{ct} versus θ_o was only 14 W m^{-2}, which is within about 2% of the mean flux at typical stratus cloud-top levels and shows that the cloud-top flux is rather insensitive to the upper-atmospheric temperature and humidity profiles.

The diagonal line in Fig. 5 represents perfect agreement between the predicted and measured fluxes, and the scatter about this line indicates the degree of the combined uncertainty of the predictions and measurements. On the average, the difference $F_p - F_g$ is -4.3 W m^{-2}; the residual standard deviation is 30.6 W m^{-2}. Taken relative to the mean cloud top flux of 774 for these 61 cases, the mean difference is on the order of about 0.5% ± 4%.

To better understand the uncertainties evident in the results above, an analysis of the sensitivity of T_c to uncertainties in cloud albedo was undertaken. It was found that large uncertainties in α_d result in small differences in the calculation of T_c. For instance, a 15% increase (decrease) in cloud albedo translates into less than a -2% ($+2\%$) change in estimates of cloud transmissivity when (2) is used. Despite this insensitivity, large errors in parameterized cloud radiative properties are manifest in the low LWP region. The slopes of the curves presented in Fig. 3 all change by an order of magnitude over a small range of LWP in which the measurements of LWP are least reliable.

c. *Sensitivity to ice content*

Even during the summer months, cloud ice may form, especially at the top of thick clouds. Also, past lidar measurements have shown that high-level cirrus clouds exist climatologically about 40% of the time during Colorado summer days (Lerfald et al. 1980). Cloud ice is not detected by the microwave radiometer. If ice is present, the total water–ice content would obviously be underestimated, and the additional attenuation by this ice would not be accounted for in our calculations of T_c.

By comparing time series analyses of GOES IR brightness temperatures to the radiosonde-derived cloud-top temperatures, a determination of the possible presence of cirrus was made. Image sectors were chosen, centered on the Denver WSFO site, to include the most significant part of the pyranometer's field of view (within a radius of 16 km). If the difference between the area mean IR brightness temperature (taken to approximate the cloud-top temperature) and the radiosonde-derived temperature exceeded -12°C, moderately thick cirrus was assumed to be present above the stratus layer. A comparative analysis of ice and no-ice cases revealed essentially no effects of significance on the conclusions of this paper. Thus, ice effects are small (at least in the cases involving cirrus), as was also noted by Griggs (1968). Errors due to the uncertainties in estimating F_{ct} or in the measurement of either F_g or

ILWC are at least as large as the differences illustrated in Fig. 4. These other sources of error are discussed in section 6.

d. Further considerations regarding parameter uncertainties

Table 3 summarizes the sensitivity of Wiscombe's six-parameter model to uncertainties in the critical variables needed to solve (1). Errors due to uncertainties in the parameterization of α_d are negligible in the context of the analysis method discussed above. Although transmissivity tends to decrease with increasing cloud albedo, multiple reflections below the cloud tend to enhance F_g to compensate for this additional cloud attenuation. Assuming that the albedo parameterization is correct, we next considered what effect uncertainties in measurements of LWP obtained operationally might have on F_p. By means of the albedo parameterization, an assumed accuracy of 10% (Hogg et al. 1983) leads to about 4% uncertainty in predicted flux. We also considered fairly large uncertainties with regard to surface albedo and found that, on the average, a 20% error in ρ translates into less than a 3% error in F_p since these uncertainties affect only terms involving multiple reflections.

Of course, the largest and most direct influences on the prediction of surface flux are related to the factors appearing in the numerator of (1). Percentage errors in any one of these variables result in equivalent errors in F_p. Listed in Table 3 are the typical uncertainties and resultant errors expressed both in terms of relative percentage differences from normal calculations of F_p and typical flux differences, assuming a cloud-top flux of 774 W m^{-2} (found to be the mean for the 61 days under consideration).

The magnitudes of these errors are such that climate sensitivity to small perturbations in total liquid water path causing changes in cloudiness, or to changes in trace gas or aerosol concentrations or surface albedo, would not be detectable. Nonetheless, the use of the proposed parameterizations in conjunction with a simple radiative transfer model such as Wiscombe's multiple reflection model may be very useful not only for developing more accurate climate change scenarios but also for improving long-range weather forecasts through a more realistic treatment of cloud radiative effects.

6. Conclusions

The objective of finding an empirical relationship between the transmissivity of continental stratiform water clouds and ILWC has been accomplished by the combination of an extensive dataset and available radiative transfer models. Figure 3 is the result of this effort. The usefulness of this parameterization depends on two factors: the goodness of the empirical fit (Fig. 3) and the high sensitivity of T_c at low values of LWP to errors of measurement and analysis techniques.

The residual standard deviation of the parameterization is 0.041, suggesting that solar attenuation by stratus clouds may be approximated within ±4% if estimates of ILWC by satellite measurement can be made to substantial accuracy. However, this estimate of accuracy is an average over a limited range of liquid water path. The data used in the analysis range from $0.1 \leqslant \text{LWP} \leqslant 2.0$ mm for zenith angles less than 50°. Cloud albedo increases while transmissivity decreases very rapidly for slight increases in LWP at low values of water content. These changes occur at the threshold of the microwave radiometer's sensitivity and are below the absolute accuracy of the retrieval technique (Hogg et al. 1983). This is a familiar problem faced in any satellite-based cloud measurements when clouds are optically thin or broken. In addition, as we have dis-

TABLE 3. Sensitivity of the six-parameter predictive model to uncertainties in critical parameters.

Parameter	Uncertainty (% change)	Rel % difference in F_g	Flux change (W m^{-2})	Uncertainty attributed to
Cloud albedo (α_c)	+15	+0.25	+2	satellite calibrations &
	−15	−0.22	−2	parameterization RSD†
Liquid water path (LWP)	+10	−3.7	−29	accuracy of μW-radiometer
	−10	+4.4	+34	
Surface albedo (ρ)	+20	−2.7	−21	differences in BAO & WSFO
	−20	+2.6	+20	surface types
Cloud trans. (T_c)	±5	±5.0	±39	RSD of empirical fit (see Fig. 4)
Cloud-top flux (F_{ct})	±3	±3.0	±23	variable cloud height, atmospheric effects, above stratus, cirrus cloud effects

* Assumes a mean cloud-top flux of 774 W m^{-2}.
† RSD = residual standard deviation.

cussed, there are clearly other degrees of freedom in the dataset that are associated with cloud microphysics.

Despite such technical limitations, we believe that simple parameterizations of bulk radiative properties such those which we have used here in Eqs. (3) and (4) must be developed further and tested for possible use in climate models. The use of empirical relationships in conjunction with a simple predictive radiative transfer model such as Wiscombe's may provide numerically efficient and reasonably accurate simulations of surface flux. Empirically derived methods have the advantage over theoretical ones in that they inherently incorporate effects of natural cloud inhomogeneities. It must be emphasized, however, that the results reported here are subject to the assumptions stated above. More complicated spatially inhomogeneous and temporally varying cloud systems, particularly multiple layer cloud systems, and clouds containing mixtures of ice and water particles, must still be treated.

Both theory and the data discussed in this article support the shapes of the curves in Fig. 3, with LWP as the important variable affecting the clouds' transmissivity, absorptivity, and albedo. For stratus clouds, there is a rapid decrease of T_c, and rapid increases of a_c and α_c, with increasing LWP for small values (0.0–0.01 mm) of LWP. As LWP becomes larger ($> \sim 0.4$ mm), these three quantities change slowly. Therefore, stratus clouds with larger values of LWP can increase or decrease in LWP considerably without significantly affecting cloud radiative properties in the visible spectrum. On the other hand, for clouds of very low optical thickness, small changes in LWP will dramatically alter the radiative properties of the clouds. This has important implications for the atmospheric radiation balance in circumstances of changing atmospheric water content. It must be further studied whether this role of stratus clouds in the climate system is, in some averaged sense, applicable to world-wide cloudiness.

Acknowledgments. The authors are grateful to Melinda Trizinski, Kathryn Jaeger, and Suchi Psakaros for their programming and data processing assistance. We wish to thank Martin Decker for providing processed radiosonde data and suggestions for interpreting the microwave radiometer data. Jim Jordan and Dave Merritt were mainly responsible for assuring that accurate and continuous radiometric data were acquired and Don Nelson kindly performed periodic calibrations of the Stapleton pyranometer. Satellite imagery was provided by Garrett Campbell and John Augustine, and aerosol optical depth data were made available thanks to Pat Reddy. We are particularly grateful to Si-Chee Tsay for providing the discrete-ordinate code and to a number of people who made many useful suggestions during the course of this study, including Ellsworth Dutton, Bob Cess, and Warren Wiscombe. One of us (HPH) would like to acknowledge NASA's Langley Research Center for support through its Grant No. NAG-1-651 to the University of Colorado.

APPENDIX

List of Symbols

a_c	Cloud absorptivity
A, B	Regression coefficients for cloud albedo
C, D	Regression coefficients for cloud transmissivity
F_{ct}	Broadband solar flux incident at cloud top
F_g	Downward solar flux at ground
F_p	Predicted downward solar flux at surface
F_s	Simulated downward solar flux at surface
T_c	Cloud transmissivity
T_{cg}	Subcloud layer transmissivity
α_c	Cloud-top albedo
α_d	Cloud-base ableda
α_{cg}	Albedo of the subcloud layer
μ_0	Cosine of solar zenith angle
ρ	Surface albedo
θ_0	Solar zenith angle

REFERENCES

Askne, J. I. H., and E. R. Westwater, 1986: A review of ground-based remote sensing of temperature and moisture by passive microwave radiometers. *IEEE Trans. Geosci. Remote Sens.*, **GE-24,** 340–348.

Coakley, J. A., Jr., and J. B. Snider, 1989a: Observed reflectivities and liquid water content for marine stratocumulus. Preprint volume, *Symposium on the Role of Clouds* in *Atmospheric Chemistry and Global Climate,* Anaheim, CA, Amer. Meteor. Soc., 175–177.

——, and ——, 1989b: Observed cloud reflectivities and liquid water paths—an update. Extended Abstracts, *FIRE Science Meeting,* Monterey, CA, FIRE Project Office, NASA Langley Research Center, 63–66.

Derr, V. E., and H. P. Hanson, 1984: Experimental optical and microphysical properties of clouds pertinent to radiative transfer. *IRS '84: Current Problems in Atmospheric Radiation,* G. Fiocco, Ed., A. Deepak Publishing Inc., 167–170.

Dutton, E. G., 1989: Annual forcing of the surface radiation balance diurnal cycle as measured from a high tower near Boulder, CO. *J. Climate,* (1990), **3** (12), 1400–1408.

——, J. J. DeLuisi, and D. J. Endres, 1985: Solar radiation at the Barrow, AK, GMCC baseline observatory. NOAA Data Report ERL ARL-6, Air Resources Laboratory, Silver Spring, MD.

Griggs, M., 1968: Aircraft measurements of albedo and absorption of stratus clouds and surface albedos. *J. Appl. Meteor.,* **7,** 1012–1017.

Hogg, D. C., F. O. Guiraud, J. B. Snider, M. T. Decker and E. R. Westwater, 1983: A steerable dual channel microwave radiometer for measurement of water vapor and liquid in the troposphere. *J. Climate Appl. Meteor.,* **22,** 789–806.

Lerfald, G. M., V. E. Derr, N. L. Abshire, R. E. Cupp and H. L. Erikson, 1980: Optical properties of clouds and aerosols derived from ground-based remote sensing methods. *Role Electro-Optics Photovoltaic Energy Conversion. SPIE,* **248,** 166–171.

Liou, K.-N., and G. D. Wittman, 1979: Parameterization of the radiative properties of clouds. *J. Atmos. Sci.,* **36,** 1261–1273.

Myers, D. R., Uncertainty analysis for thermopile pyranometer and pyrheliometer calibrations performed by SERI. SERI/TR-215-3294, Solar Energy Research Institute, U.S. Dept. of Energy, Golden, CO, 29 pp.

Pandey, P. C., E. G. Njoku, and J. W. Waters, 1983: Inference of

cloud temperature and thickness by microwave radiometry from space. *J. Climate Appl. Meteor.*, **22,** 1894–1898.

Ramanathan, V., R. D. Cess, E. F. Harrison, P. Minnis, B. R. Barkstrom, E. Ahmad and D. Hartmann, 1989: Cloud-radiative forcing and climate: results from the Earth Radiation Budget Experiment. *Science,* **243,** 57–63.

Slingo, A., 1989: A GCM parameterization for the shortwave radiative properties of water clouds. *J. Atmos. Sci.,* **46,** 1419–1427.

——, and H. M. Schrecker, 1982: On the shortwave radiative properties of stratiform water clouds. **108,** 407–426.

Staelin, D. H., K. F. Kunzi, R. L. Pettyjohn, R. K. L. Poon and R. W. Wilcox, 1976: Remote sensing of atmospheric water vapor and liquid water with the Nimbus 5 microwave spectrometer. *J. Appl. Meteor.,* **15,** 1204–1214.

Stamnes, K., S.-C. Tsay, W. Wiscombe and K. Jayaweera, 1988: Numerically stable algorithm for discrete-ordinate-method radiative transfer in multiple scattering and emitting layered media. *Appl. Opt.,* **27,** 2502–2509.

Stephens, G. L., 1978: Radiation profiles in extended water clouds. II: Parameterization schemes. *J. Atmos. Sci.,* **35,** 2123–2132.

——, 1979: Optical properties of eight water cloud types. Division of Atmospheric Physics Technical Paper No. 36, Commonwealth Scientific and Industrial Research Organization, 35 pp.

——, S. Ackerman, and E. A. Smith, 1984: A shortwave parameterization revised to improve cloud absorption. *J. Atmos. Sci.,* **41,** 687–690.

Tsay, S.-C., K. Stamnes, and K. Jayaweera, 1989: Radiative energy budget in the cloudy and hazy Arctic. *J. Atmos. Sci.,* **46,** 1002–1018.

Wiscombe, W. J., 1975: Solar radiation calculations for Arctic summer stratus conditions. *Climate of the Arctic,* Geophysical Institute, Univ. of Alaska, Fairbanks, 245–254.